Development and Applications of Kramers-Kronig PEELS Analysis Software

by

X.D. Fan*, J.L. Peng, and L.A. Bursill**

School of Physics, University of Melbourne,
Parkville, 3052, Vic., Australia

* Present address: Department of Materials and Metallurgy, Cambridge University,
Pembroke Street, Cambridge, U.K. CB2 3QZ

Abstract

A Kramers-Kronig analysis program is developed as a custom function for the GATAN parallel electron energy loss spectrascopy (PEELS) software package EL/P. When used with a JEOL 4000EX high-resolution transmission electron microscope this program allows us to measure the dielectric function of materials with an energy resolution of approx 1.4 eV. The imaginary part of the dielectric function is particularly useful, since it allows the magnitude of the band gap to be determined for relatively wide-gap materials. More importantly, changes in the gap may be monitored at high spatial resolution, when used in conjunction with the HRTEM images. The principles of the method are described and applications are presented for a Type 1a gem quality diamond, before and after neutron irradiation. The former shows a band gap of about 5.8 eV, as expected, whereas for the latter the gap appears to be effectively collapsed. The core-loss spectra confirm that Type 1a diamond has pure sp^3 tetrahedral bonding, whereas the neutron irradiated diamond has mixed sp^2/sp^3 bonding. Analysis of the low-loss spectra for the neutron-irradiated specimen yielded density 1.6 g/cm^3, approximately half that of diamond.

** Corresponding author:
L.A. Bursill, School of Physics, University of Melbourne
Parkvile, VIC 3052, Australia.
email: bursill@physics.unimelb.edu.au
Fax: 61.3.93474783
Phone: 61.3.93447651/5431

Subject keywords: Kramers-Kronig Analysis/KKA
Electron energy loss spectroscopy/PEELS
High-resolution transmission electron microscopy/HRTEM

1. Introduction

Kramers-Kronig analysis of PEELS data is desirable in order to obtain the real and imaginary parts of the dielectric function, as well as the optical absorption coefficient and "effective electron numbers" [1-3]. Kramers-Kronig analysis (KKA) enables the energy dependence of the real part (ϵ_1) and the imaginary part (ϵ_2) of the permittivity to be calculated from the energy loss function, which is performed according to the method of Johnson [4-6]. There exists the possibility of obtaining additional information which may be helpful in measuring the band gap and detecting the presence of interband transitions. Our Gatan PEELS analysis software did not perform this analysis satisfactorily. This paper describes the development of software suitable for Macintosh personal computers in our laboratory.

Care was taken with deconvolution of the zero-loss peak and multiple scattering events, in order to first obtain the single scattering loss function. The analysis for the dielectric function was then performed according to standard methods [1-3], using sinusoidal Fourier transforms and an inverse cosinusoidal F.T. as suggested by Johnson [4-6]. The KKA analysis was written in C using the Macintosh Programming Workshop (MPW). It is thus inserted as a Custom Function in the GATAN EL/P program.

Examples of applications will be presented, including the determination of the band gap of Type 1a diamond before and after neutron irradiation. Although the resolution of the energy loss spectrometer is limited to 1.4 eV, the results are nevertheless interesting for relatively wide-gap materials of current and future interest, such as diamond varieties, aluminum-nitrides and some silica-derived glasses. Furthermore, we may combine high spatial resolution HRTEM results, which allow the structural textures to be characterized, with the PEELS/KKA analysis of the low-loss and core-loss spectra, which may provide useful information concerning the nature of the chemical bonding and mass density, as well as the dielectric response.

2. Principles of Kramers-Kronig Analysis

Although the principles for this technique were developed some 25 years ago [1], they may not be familiar to current users of PEELS techniques. Probably, this situation is due to the relatively low energy resolution of the spectrometers in use with HRTEM instruments (say 0.5 - 1.5 eV). This is certainly a major limitation for most materials; however, we propose that there is a valid range of applications for materials scientists which concerns current interests in relatively wide-gap materials. A brief statement of the principles of the method follows, the interested reader may consult Refs. [1-3] for more complete treatments.

The single-scattering distribution (SSD) is related to the complex permittivity or the dielectric function ϵ as:

$$S(E) = \frac{I_0 t}{\pi a_0 m_0 v^2} \mathrm{Im}[-1/\epsilon(E)] \ln[1 + (\beta/\theta_E)^2] \qquad (1)$$

where I_0 is the zero loss intensity, t the specimen thickness, v is the electron beam velocity, β is the collection semi-angle and $\theta_E = E/(\gamma m_0 v^2)$ is the characteristic scattering angle for

energy loss E. γ is the relativistic factor, a_0 is Bohr radius and m_0 is the electron mass.

Based on the fact that the dielectric function is causal, it can be shown that there is a relation between the real and imaginary parts, known as the Kramers-Kronig transformation:

$$\mathrm{Re}\left[\frac{1}{\epsilon(E)}\right] = 1 - \frac{1}{\pi} P \int_0^\infty \mathrm{Im}\left[\frac{-1}{\epsilon(E')}\right] \frac{E' dE'}{E'^2 - E^2} \tag{2}$$

where P is the Cauchy principal part of the integral.

The above transformation is known as the integration method, as the whole range of Im[-1/$\epsilon(E')$] is integrated for each point of Re[1/$\epsilon(E)$]. Therefore it is a time comsuming algorithm from the computational point of view. Johnson [4-6] introduced an equivalent Fourier transform method. Instead of integration, we first take the direct sine transformation and then an inverse cosine transformation. Unless the specimen thickness is known exactly, we need to determine the proportionality constant in Eq.(1). Applying the Kramers-Kronig sum rule at $E = 0$ we obtain:

$$1 - \mathrm{Re}\left[\frac{1}{\epsilon(0)}\right] = \frac{2}{\pi} P \int_0^\infty \mathrm{Im}\left[\frac{-1}{\epsilon(E)}\right] \frac{dE}{E} \tag{3}$$

where $\epsilon(0) = n^2$ and n is the refractive index.

Alternatively, using the Bethe sum rule we have:

$$\int_0^\infty \mathrm{Im}\left[\frac{-1}{\epsilon(E)}\right] E dE = \frac{\pi}{2} E_p^2 \tag{4}$$

where E_p is the plasma energy loss peak.

Therefore, knowing either the refractive index or the plasma peak, the proportionality constant K can be determined in Eq.(1):

$$K = I_0 t / \pi a_0 m_0 v^2 \tag{5}$$

Thus as an extra result of KKA, the absolute specimen thickness may be determined, at least in principle. Once the proportionality constant is known, Im[1/$\epsilon(E)$] is readily available from Eq.(1), then we can calculate Re[1/$\epsilon(E)$] by Eq.(2).

Consequently, we can derive the real and imaginary parts of the dielectric function (ϵ_1, ϵ_2):

$$\begin{aligned} \epsilon(E) &= \epsilon_1(E) + i\epsilon_2(E) \\ &= \frac{\mathrm{Re}[1/\epsilon(E)] + i\mathrm{Im}[-1/\epsilon(E)]}{\{\mathrm{Re}[1/\epsilon(E)]\}^2 + \{\mathrm{Im}[-1/\epsilon(E)]\}^2} \end{aligned} \tag{6}$$

For convenience we include the following glossary for the various parameters referred to in the KKA.

Glossary of Parameters used for the KKA

$\epsilon(E)$	: complex dielectric constant.
ϵ_1	: real part.
ϵ_2	: imaginary part.
I_0	: zero loss intensity.
t	: specimen thickness.
β	: collection semi-angle.
θ_E	: characteristic scattering angle $E/(\gamma m_0 v^2)$
γ	: relativistic factor.
a_0	: Bohr radius.
m_0	: electron mass.
v_0	: electron velocity.

3. Software Development

To develop a program as a custom function of the Gatan EL/P package, the basic requirements are the Gatan EL/P package with EL library and the Macintosh Programing Workshop (MPW) with C or Pascal language compiler. Our source code was written in C language.

We have used both the integration (Eq.(1) and an equivalent Fourier transform method. The integration method has a much longer computation time, especially for a large number of channels. However it allows us to verify the reliability of the Fourier method. This is important because the numerical methods for fast Fourier transforms may be quite tricky, especially when they involve the sine and cosine transforms. Both the K-K and Bethe sum rules were used to determine the proportionality constant K. The Bethe sum rule is usually prefered as the plasmon peak energy can be easily obtained from the low energy loss data.

To instal the program, the compiled KKA module is simply placed in the EL/P folder. Requests for the software may be addressed to the first author.

4. Experimental and Analysis

Our primary results were obtained using a Gatan Parallel Detection Electron spectrometer (Model 666) attached to the JEOL-4000EX electron microscope. The resolution of the spectra was determined by measuring the full width at half-maximum (FWHM) of the zero-loss peak; this was typically close to 1.4eV when the JEOL-4000EX was operated at 100kv. All PEELS data referred to here were recorded at 100kV. The HRTEM images were recorded at 400keV. Note that our JEOL 4000EX instrument has been successfully configured to allow rapid switching between 400 keV and 100 keV operation.

All spectra were collected at identical convergence and collection angles and were typically measured from areas of about 120nm in diameter, recording times were 120s for core loss and 0.3s for low loss. Spliced segment processing was often used to piece together a continuous

spectrum from two segments of spectra acquired over low and higher energy-loss ranges.

HRTEM images and PEELS spectra from a variety of carbon-based materials were acquired under identical condition; referred to in this paper is a Type 1a diamond, both before and after it was given a dose of 1.632 x 10^{21} nvt, when its density decreased from 3.52 to 1.9 g/cm^3 (see Ref. [7].

Specimens for electron microscopy were prepared by simply placing clean, dry freshly crushed diamond powders onto a 1000 mesh copper grids. This technique significantly reduces electron beam irradiation damage and chemical contamination of the specimens during observation.

HRTEM was used to select areas which appeared relatively homogeneous and of slowing increasing thickness. Images were recorded using a JEOL-4000EX electron microscope operating at 400keV; the spherical aberration coefficient of the ultra-high resolution pole-pieces was Cs=0.94mm and the effective Scherzer or interpretable image resolution is 0.17nm. The specimen height was carefully adjusted to an optimum focussing current, when the objective lens astigmatism as well as the optical alignment parameters could be set precisely against calibrated values. PEELS data were rejected unless there was no apparent microstructual damage or specimen contamination over the area being illuminated by the electron beam; this was monitored by comparing images before and after recording the electron energy loss spectra.

All spectra were deconvoluted to obtain the single scattering distribution (SSD) using the Fourier-Log method [2]. The zero-loss peaks were removed by fitting a symmetric zero-loss peak to the negative-energy tail in each of the spectra. Both these processes were carried out using the standard Gatan EL/P software (version 2.1.1). The zero-loss peak was stored as an equivalent delta function in the first channel of the SSD.

Next, the KKA analysis was performed as follows: the proportionality constant (K) and consequently the thickness (t) were then calculated using a sum rule; thus the loss function Im(-1/ϵ) could be obtained. Then the KKA transform (Eq.2) was applied to obtain Re(-1/ϵ). The real and imaginary parts of the dielectric function (ϵ_1, ϵ_2) were then calculated using Eq.(6) above. For completeness, the optical absorbtion coefficient (μ) and an appropriate part of the core-loss spectrum were also included as part of our standard output results for a typical KKA analysis (see e.g. Figs.1,2).

5. Results

Figs.1 and 2 show our standard KKA output results for the Type 1a diamond and the neutron irradiated diamonds respectively. For the former (Fig.1) the SSD, the loss function and the dielectric functions (ϵ_1, ϵ_2) are very much as expected for gem quality diamond (c.f. Fig. 25 of Ref. [3]). Note especially the result for ϵ_2, which shows clear evidence for the band gap of diamond (about 5.8 eV). The absence of a π plasmon peak is typical of pure sp^3 diamond-like materials. This is confirmed by the core loss portion of the PEELS (inset bottom right corner of Fig.1), which shows no sign of the edge structure typical of sp^2 carbons (c.f Fig.25 of Ref. [3]).

The neutron irradiated diamond (Fig.2) showed quite different results; thus the SSD

and the loss function both show a small peak at about 6 eV, corresponding to the π -π^* transition of sp^2-type graphitic carbons, as well as the σ to σ^* transition at about 13 eV. In this case the corresponding core loss portion of the PEELS (inset bottom right of Fig.2) shows edge structure about 285-295 eV typical of graphitic or sp^2-type carbons. Similarly the dielectric functions (ϵ_1, ϵ_2) derived by KKA analysis are consistent with the results of Fink for graphite (c.f. Fig.25 of Ref. [3]); note especially that the band gap of the neutron irradiated diamond has collapsed significantly relative to that of the original diamond. Analysis of the plasmon peak position (Fig.2) relative to the corresponding results for diamond and graphite yielded density 1.6 $g.cm^{-3}$, which should be compared with the density reported by direct measurement [7]. It is also comparable to typical glassy carbons or nanoporous carbons [9].

6. Discussion

For semi-metallic structures, such as graphite, the band gap is too small to be measured with our current resolution of about 1.4 eV. Therefore, at this stage, the KKA method can only measure wide band-gaps for insulating materials like diamond (see Fig.1 above). Again the electron energy loss techniques have lower resolution than optical methods. However, it does have its own advantages. Firstly, it covers a wider energy range which may include the ranges covered by visible, ultraviolet and soft x-ray radiation. Second, in combination with high resolution electron microscopy, it allows the structure of localized regions to be characterized, along with their PEELS spectra. The low energy resolution gives rise to difficulties near the zero-loss region. This can be overcome only by increasing the instrumental resolution as well as being extremely careful with a zero-loss simulation to obtain more accurate single scattering distributions. It was also apparent that the KKA proceeded satisfactorily only for relatively noiseless data sets. Thus, there may be some difficulties using this analysis for data obtained using nanoprobe instruments. Use of the relatively large probe diameter characteristic of HRTEM may yield relatively noise-free data; it also induces relatively less electron induced irradiation damage.

7. Conclusion

In this paper we have presented some simple results which illustrate some of the potential applications of KKA analysis of PEELS for materials having relatively wide band gaps. Results for a nanoporous amorphous carbon (NAC) have been reported elsewhere [9]. Thus, we were able to show that the electronic state of this material was essentially semi-metallic, by comparison with highly oriented pyrolytic graphite (HOPG), evaporated amorphous carbon (EAC), glassy carbon (GC), C_{60} and a CVD diamond. Results for a series of ten neutron irradiated samples [10] are also in press and studies of some wide-gap silica-based glasses as well as Al-N are also in preparation.

Acknowledgements

The authors wish to thank Australia Research Council for financial support of this project. X.D. Fan is grateful for the award of an ARC Postdoctoral Research Fellowship (1993-5). We thank Dr. Lou Vance, Dr Judith Milledge and Dr. Monica Mendelsohn for providing the diamond specimens.

REFERENCES

1. J. Daniels, C. von Festenberg, H. Raether and K. Zeppenfeld, *Springer Tracts in Modern Physics*, **54**, 72-135 (1970).
2. R.F.Egerton, *Electron Energy Loss Spectroscopy in the Electron Microscope*, New York, (1986).
3. J.Fink, *Advances in Electronic & Electron Physics*, **75**, 121-231 (1989).
4. D.W. Johnson, *J. Phys. A:Maths and Gen.,*, **8**, 490-495 (1975).
5. D.W. Johnson and J.C.H. Spence, *J. Phys.*, **D7**, 771-780 (1974).
6. D.W. Johnson, PhD Thesis, University of Melbourne (1976).
7. D.T. Keating, *Acta Crystallogr.*, **16**, A113-A114 (1963).
8. S.D.Berger, D.R.McKenzie and P.J. Martin, *Phil. Mag. Lett.,*, **57**, 285-290 (1988).
9. J.L.Peng, X.D.Fan and L.A. Bursill, *Inter. J. Mod. Physics. B*, in press (1996).
10. J.L. Peng and L.A. Bursill, *submitted*, (1996).

FIGURE CAPTIONS

Figure 1
Typical KKA analysis of PEELS for gem quality Type 1a diamond. Note band gap of about 5.8 eV evident in Im[ϵ].

Figure 2
Typical KKA analysis of PEELS for Type 1a diamond after neutron irradiation dose of 1.632 x 10^{21} nvt. Note collapse of band gap evident for Im[ϵ], c.f. corresponding result in Fig.1.

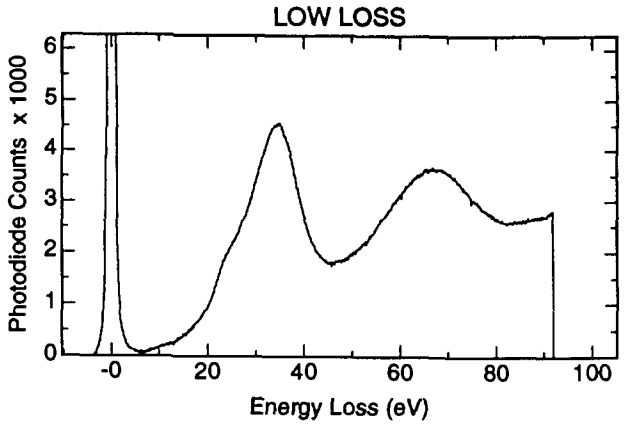
LOW LOSS
Photodiode Counts x 1000
Energy Loss (eV)

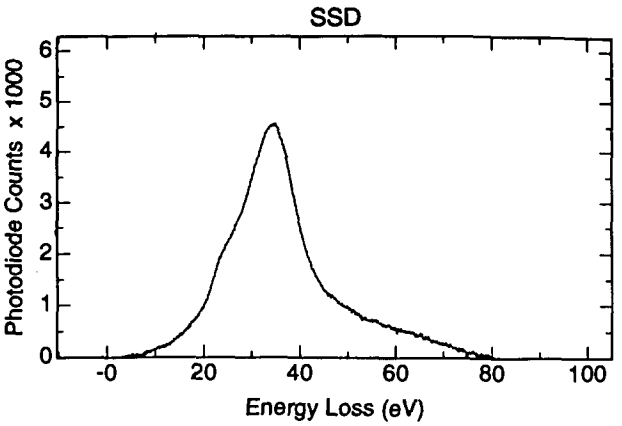
SSD
Photodiode Counts x 1000
Energy Loss (eV)

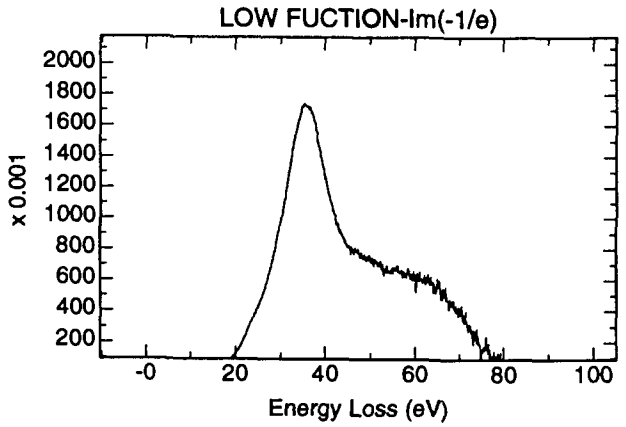
LOW FUCTION-Im(-1/e)
x 0.001
Energy Loss (eV)

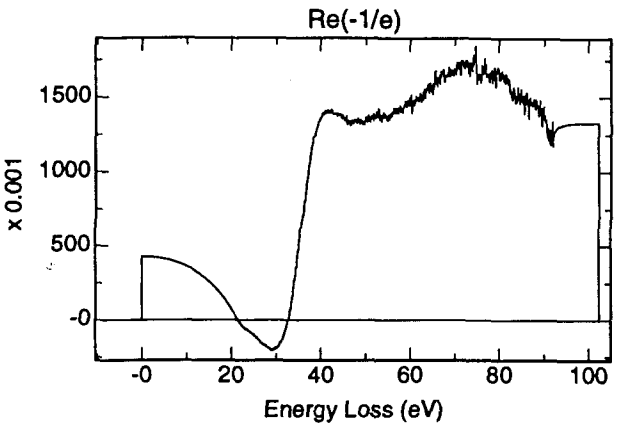
Re(-1/e)
x 0.001
Energy Loss (eV)

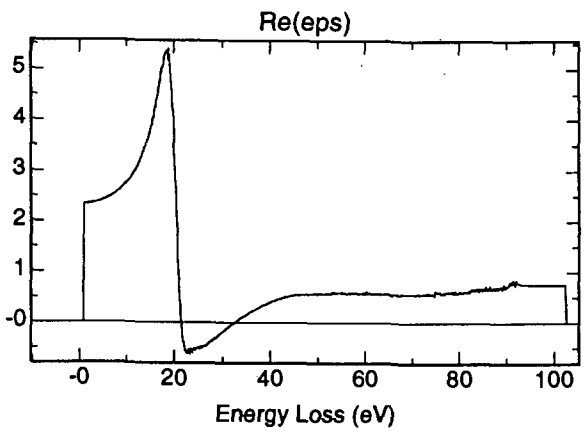
Re(eps)
Energy Loss (eV)

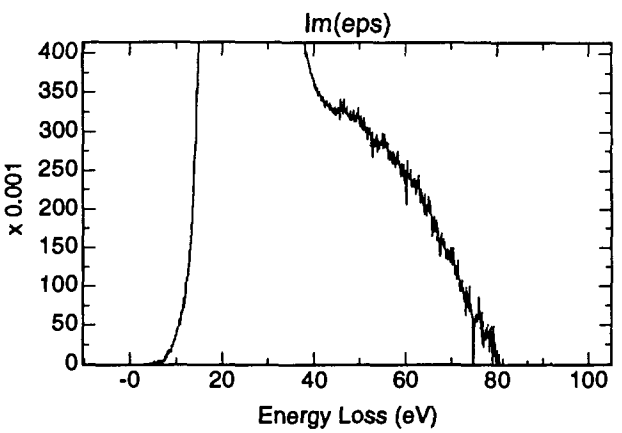
Im(eps)
x 0.001
Energy Loss (eV)

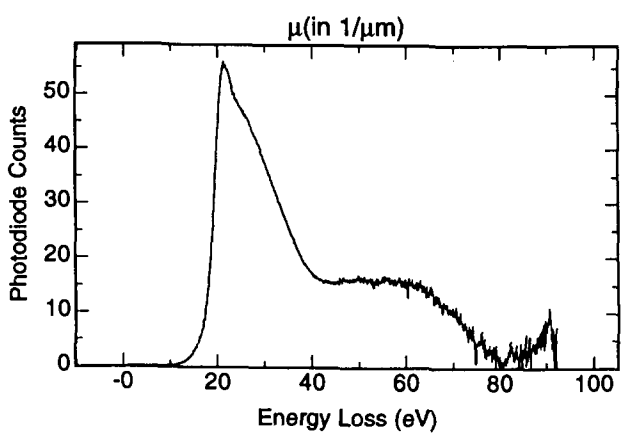
μ(in 1/μm)
Photodiode Counts
Energy Loss (eV)

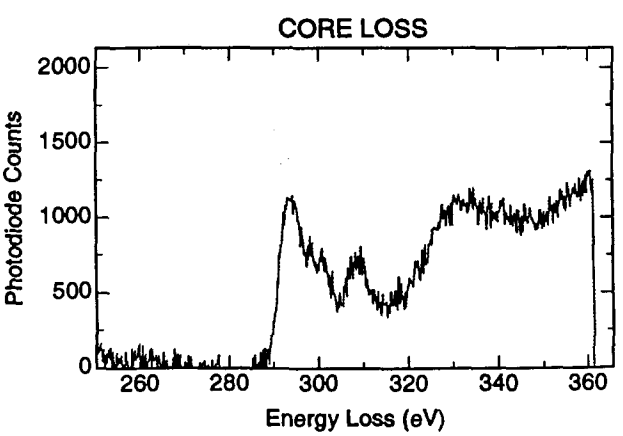
CORE LOSS
Photodiode Counts
Energy Loss (eV)

Figure 1

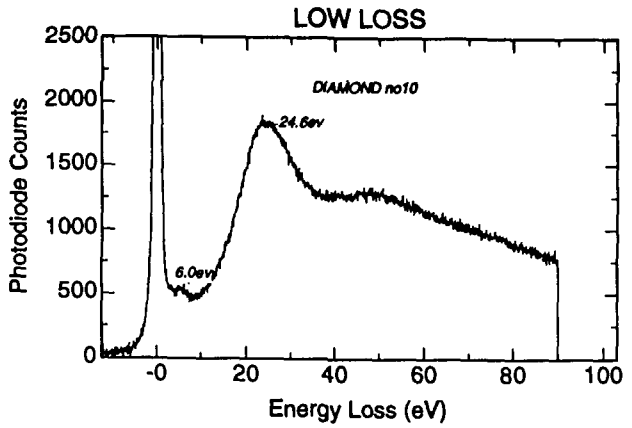
LOW LOSS
DIAMOND no10
24.6ev
6.0ev
Photodiode Counts
Energy Loss (eV)

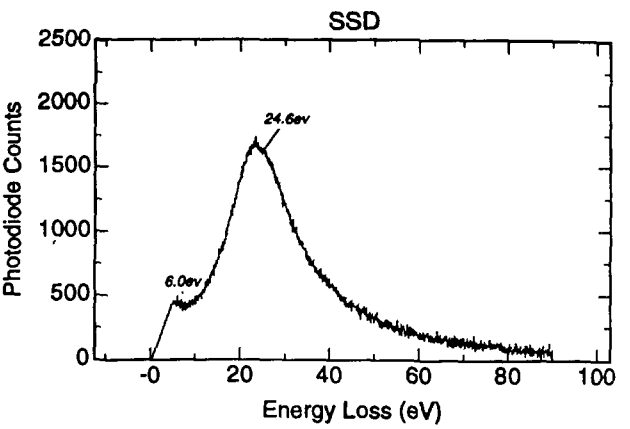
SSD
24.6ev
6.0ev
Photodiode Counts
Energy Loss (eV)

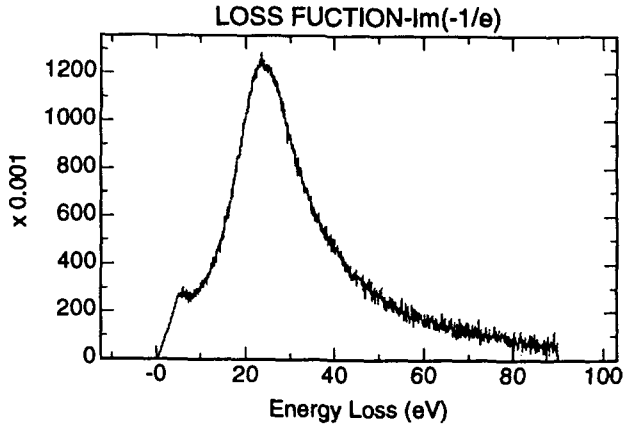
LOSS FUCTION-Im(-1/e)
x 0.001
Energy Loss (eV)

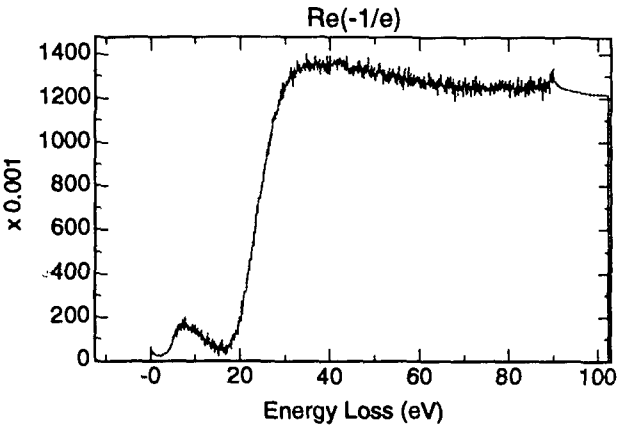
Re(-1/e)
x 0.001
Energy Loss (eV)

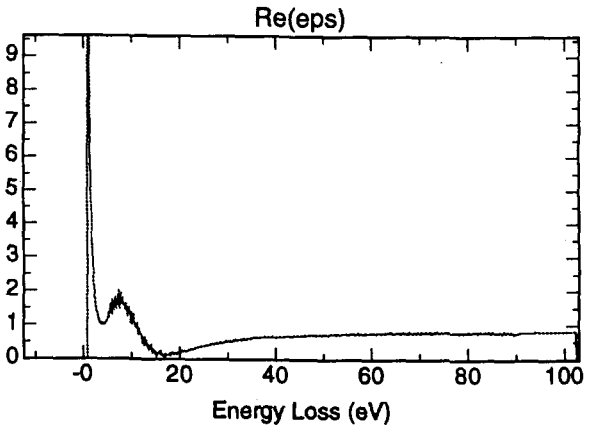
Re(eps)
Energy Loss (eV)

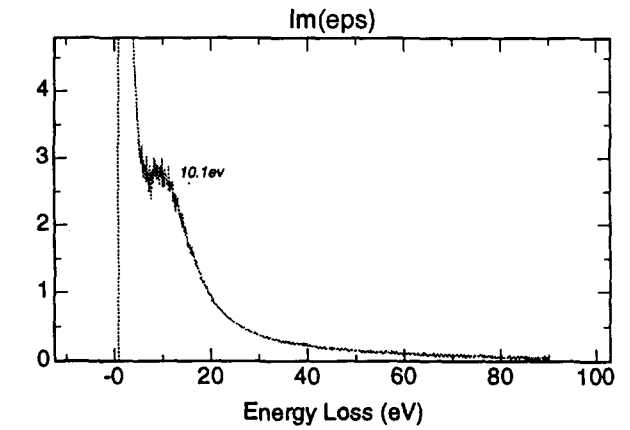
Im(eps)
10.1ev
Energy Loss (eV)

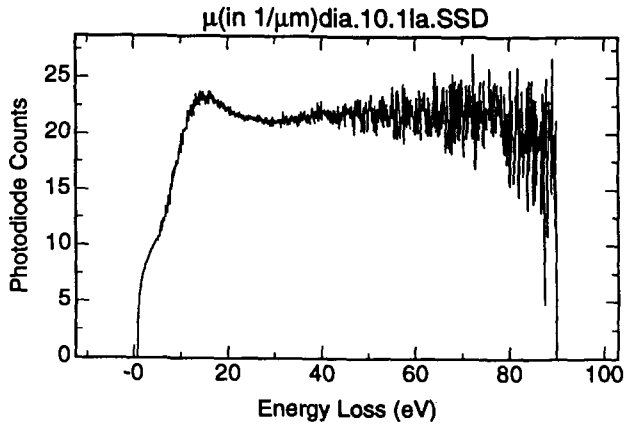
μ(in 1/μm)dia.10.1la.SSD
Photodiode Counts
Energy Loss (eV)

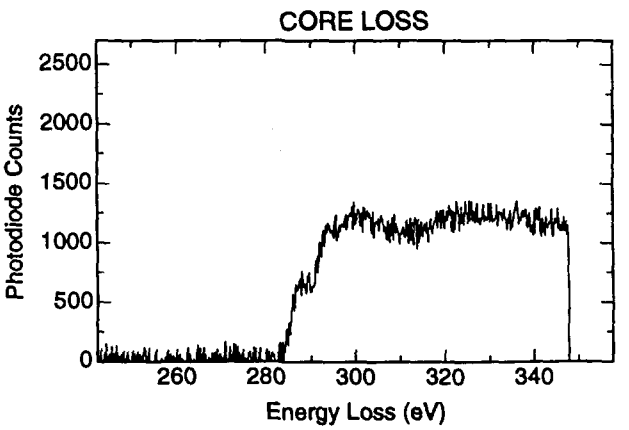
CORE LOSS
Photodiode Counts
Energy Loss (eV)

Figure 2.